Analysis of unsteady cavitating flow and pressure fluctuation around highly skewed propeller in non-uniform wake

Chao Yu, Yiwei Wang, Chenguang Huang, Xiaocui Wu, Tezhuan Du
Key Laboratory for Mechanics in Fluid Solid Coupling Systems, Institute of Mechanics, Chinese Academy of Sciences.
No.15 Beisihuanxi Road, Beijing, 100190, China
Email: yuchaohust@163.com

ABSTRACT: Numerical simulation of an unsteady cavitating flow around a highly skewed propeller in a non-uniform wake is performed based on an explicit LES approach with $k-\mu$ subgrid model. The predicted evolution of the unsteady cavitating flow and pressure fluctuation around a highly skewed propeller is in good agreement with experimental results. The relations between cavitation and pressure fluctuation are briefly analyzed based on the numerical results. Furthermore, numerical simulation of a propeller only have one blade in non-uniform wake is performed based on the same methods to analyze the relations between cavitation and pressure fluctuation clearly.

KEY WORDS: LES, cavitation, highly skewed propeller, pressure fluctuation

INTRODUCTION

In recent years, cavitating flow around the propeller is a classic issue in the hydrodynamic field. The pressure fluctuation caused by cavitation has attracted wide attention. Many difficulties are still encountered in solving this complex problem. Numerical simulation is the common method in the study of cavitating flow. In which, turbulence model is one of the key component.

For a long time, Reynolds-averaged Navier–Stokes (RANS) turbulence models are used in numerical simulations of cavitating flow. For example, Simulation of unsteady cavitating flow around a propeller based on a RANS turbulence model and the Singhal cavitation model were made by Watanabe et al. [1]. Their predicted cavity shape and pressure fluctuations were in good agreement with the obtained measurements. Simulation of the propeller cavitation with a SST turbulence model and a mass transfer cavitation model were made by Ji et al. [2,3] Their predicted cavity and pressure fluctuations were fairly consistent with experimental results. Furthermore, RANS turbulence models have been widely used in the numerical simulation of cavitating flows around more objects underwater [4-8].

In recent years, LES turbulence models are used to numerically simulate cavitation flow and achieved some progress, however, research on propeller cavitation is very limited. Lu et al. [9,10] simulated the cavitating flow around a propeller used both LES and RANS methods. In their study, more refined bubble and vortex structures had been obtained in the LES-based simulation than in the RANS-based simulation and LES was demonstrated capable of capturing the mechanisms by comparing with experimental results. In addition, numerical simulation of cavitating flow around an INSEANE779A propeller based on implicit LES was made by Bensow and Bark [11,12]. In their study, some important cavitation mechanisms were predicted, which proved the validity of the method, and they pointed out that numerical simulations of cavitating flow based on LES need further development and exploration. Furthermore, by using LES turbulence models in simulation of cavitating flows around more objects underwater, more promising results of cavity and vortex structures have been obtained [13-15].

To our knowledge, detailed numerical results of the propeller tip vortex cavitation and pressure fluctuation based on LES are particularly limited. In this study, the cavitating flow around a highly skewed propeller and one of its blade in non-uniform ship wake are numerically simulated by an explicit LES approach with $k-\mu$ subgrid model, the VOF method, Kunz cavitation model, and a moving mesh scheme. Numerical results are compared with experimental [16,17] to prove the validity of the method. Relations between cavitation and pressure fluctuation are briefly analyzed based on numerical simulation.

Numerical Simulation

In cavitating flows around a propeller [2-3,9-12] the fluid is assumed to be incompressible so that the numerical simulation is performed based on the incompressible Navier–Stokes equations. The turbulent flow are solved with an explicit LES approach with $k-\mu$ subgrid mode [18].

Cavitation Model

In the unsteady cavitation flow, the transition between liquid and vapor is complex. In this study, the mass transfer rate is based on the Kunz model [19]:

$$\dot{m}^{+}=\frac{C_v\rho_v\alpha\min[0,\bar{p}-p_v]}{(0.5\rho_l U_\infty^2)t_\infty} \quad (1)$$

$$\dot{m}^{-}=\frac{C_c\rho_v\alpha^2(1-\alpha)}{t_\infty} \quad (2)$$

The evaporation rate $\dot{m}^{+}$ is proportional to the liquid volume fraction α and the amount of local pressure subtracting the saturated vapor pressure when the pressure is below the saturated vapor pressure. The condensation rate $\dot{m}^{-}$ is modeled by a third-order polynomial function of α,. In Eq.(1), the characteristic time t_∞ is equal to D/U_∞, where D is the diameter of the propeller and U_∞ is the speed of ship. C_v and C_c are the empirical constants for the different phase transfer rates. These empirical constants are set to $C_v=100000$ and $C_c=1000$ which are based on considerable computing experience.

Study Object And Flow Parameters

A scale model of the highly skewed propeller of "SEIUN-MARU" ship[16,17] is used in this study. The major specifications of the propeller are shown in Table 1.

Table 1 Principal parameters of Propeller

Number of blades	5
Diameter at blade tip, D	0.22 m
Pitch ratio	0.955(at 0.7R)
Skew angle	45°
Rake angle	-3.03°
Expanded area ratio	0.7
Blade section	Modified SRI-B

In a Cartesian coordinate system *O-xyz*, the propeller geometry model is drawn as shown in Fig.1. The propeller only has one blade is shown as Fig.2. The *x*-axis corresponds to the propeller center rotation axis directed downstream. The *z*-axis is taken as the the blade reference line (a straight line perpendicular to the axis of the propeller and used as a vertical reference line when drawing the blade). For simplicity of presentation, the angle θ between the *z*-axis and the propeller reference line indicates the blade position during rotation.

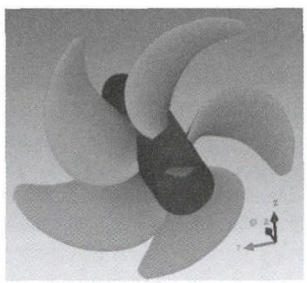

Fig. 1 Propeller geometry

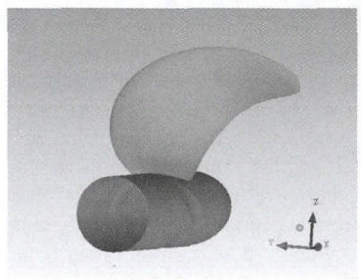

Fig.2 A propeller has one blade

Parameters of the cavitating flow are originated from published documents [16, 17]. The rotational speed n is 17.5 rps. $K_T=Thrust/(\rho_l n^2D^4)=0.201$ represents the time-averaged thrust coefficient. The distribution of measured wake velocities is shown in Fig.4. The cavitation number, $\sigma=(p_\infty-p_{sat})/(0.5\rho n^2D^2)$, is 2.99, where

$p_{sat} = 3450P_a$ is the saturation vapor pressure of water.

Computational Domain And Grids

The computational domain is prepared as shown in Fig.3, which is recommend by Ji et al.[2,3]. The inlet plane is located at $0.7D$ upstream of the propeller, and the outlet plane is located at $5D$ downstream of the propeller. The diameter of the cylindrical surface is $12D$. The moving zone is a cylindrical region: $r/D \leq 0.6$, $x/D = [-0.3, 0.2]$. The interface between the moving zone and outer zone is a split surface.

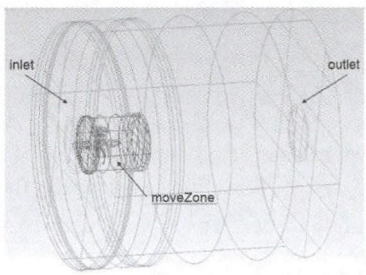

Fig. 3 Computation domain

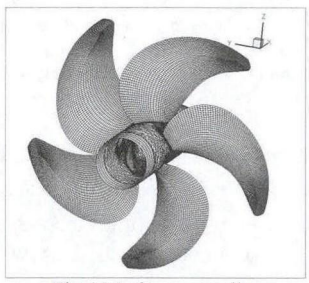
Fig.4 Mesh on propeller

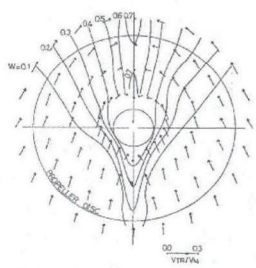
Fig.5 Measured nominal wake distribution

When the mesh is generated, the whole computational domain, as shown in Fig.3, is mainly divided into the moving zone and the outer zone by the sliding surface. The outer zone has a structured mesh with hexahedral cells. The moving zone has a multi-block mesh. The region around propeller are structured mesh with hexahedral cells as shown in Fig.4. The total grids is about 4 million cells.

Boundary Conditions

The boundary of inlet is fixed velocity. The distribution of velocity on the inlet plane is consistent with of the wake flow as shown in Fig.5, where $V_\infty = 2.79m/s$ is computed from K_T. The boundary of outlet is fixed pressure, where $P_\infty = 25700Pa$ is calculated from σ. The condition of the slip surface is set as cyclicAMI (cyclic Arbitrary Mesh Interface), which was introduced in OpenFOAM 2.1.0 [20] to enable simulation across disconnected, adjacent, mesh domains for non-conformal patches [21].

Results and Discussion

Comparison Of Numerical And Experimental Results

To validate the present numerical method, the evolution of the cavity pattern from the simulation is compared with the experimental data which is drawn from previous experimental study literatures [16, 17], as shown in Fig.6. In the simulation, we use the isosurface of vapor fraction with $\alpha_v = 0.1$ to illustrate the cavity shape which is well consist with the experimental results. The volumes of cavity on blade predicted by numerical simulation have the same changing tendency as the experimental results, as shown in Fig.7.

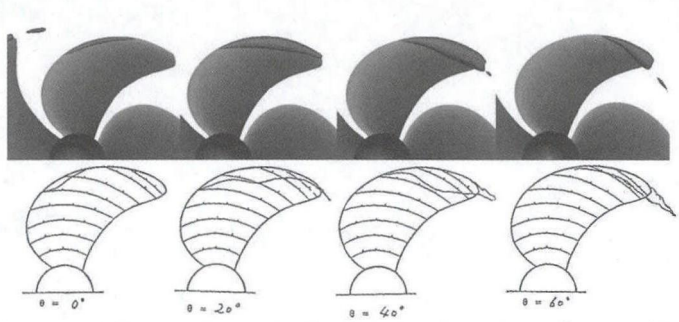

Fig.6 Evolution of the cavity pattern during propeller rotation (numerical results are in the top row, while experimental results are in the next row)

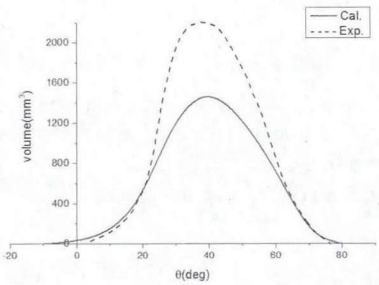

Fig.7 Comparison of cavity volume on blade

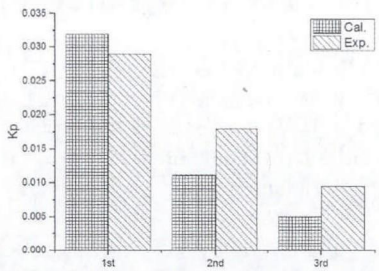

Fig.8 Comparison of the first, second and third blade frequency amplitude of K_p on point C

Around the propeller, pressure on a fixed point C are observed. The coordinate of point C is (-0.0475D, 0.744D, -0.05D). A dimensionless pressure parameters $K_p = S_p(P - p_{sat})/0.5\rho n^2 D^2$ are defined to describe the pressure fluctuation [2]. The amplitude of pressure on first, second and third blade frequency predicted by numerical simulation are well consist with experimental data, as shown in Fig.8.

Analysis of relations between cavitation and pressure fluctuation

The pressure fluctuation on point C has two peak value in every blade cycle as shown in Fig.9. At $\theta = -10°$, the pressure reaches the first peak which is also the time of cavitation inception. At $\theta = 10°$, the pressure reaches the second peak, at the same time, the cavity collapse completely on the prior blade. At $\theta = 40°$, the pressure reaches the vale while cavity volume reaches the peak. Relation to the plot of cavity volume in Fig 7, the pressure value have contrary trend with cavity value when they change with θ.

But the pressure has two peaks in a period, while the volume of cavity on the blade near the point just has one peak. Thus, the pressure on a fixed point does not only caused by the cavity value on the blade near the point. When $-10° < \theta < 10°$, point C is in the center of two blades, the pressure is effected by both the cavity on the blade where inception cavitation appear and the past blade where cavity collapse. Thus, intense pressure fluctuations effected by cavitation appear and collapse.

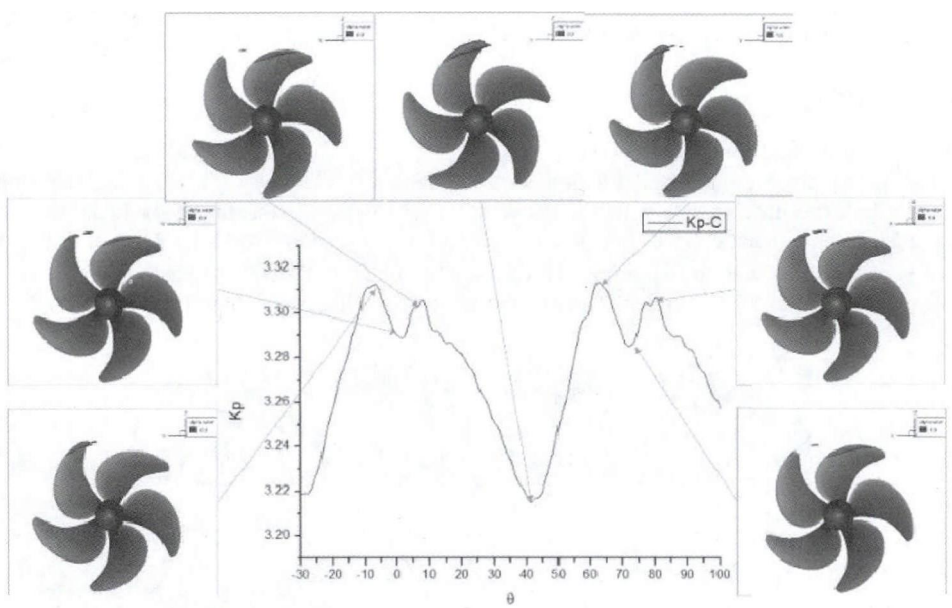

Fig.9 Relation of the pressure fluctuation on point C and the cavitation

To illustrate the relations between cavitation and pressure fluctuation more clearly, numerical simulation of a propeller only have one blade are made to analyze the relations between cavitation and pressure fluctuation clearly. However, as shown in Fig.10, the the cavity on blade are different from the past results. Although the boundary of

inlet and outlet are the same, the flow around the blade is different because the expanded area ratio decrease when there is only one blade.

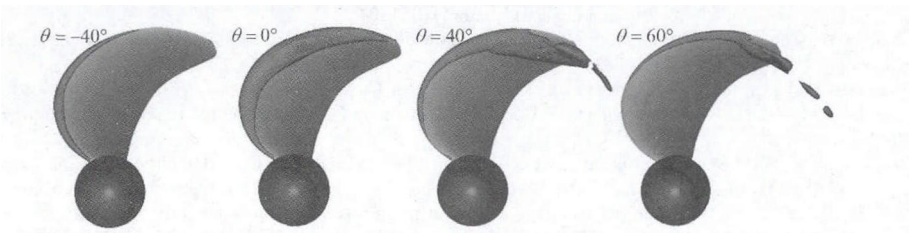

Fig.10 Evolution of the cavity pattern during propeller rotation when there is only one blade

Conclusion

In this study, numerical simulations of the cavitating flow around a highly skewed propeller and one of its blade in non-uniform ship wake are performed based on an explicit LES approach with subgrid model, Kunz cavitation model, the VOF method, and a moving mesh scheme. the predicted cavity shape and pressure fluctuations were in good agreement with the experimental results, which prove the validity of the method. Relations between cavitation and pressure fluctuation are analyzed based on numerical simulation.

When $-10° < \theta < 10°$, intense pressure fluctuations at point C is effected by both the cavity on the blade where inception cavitation appear and the past blade where cavity collapse.

The caviting flow around one blade would have a great deference without the influence of other blades. The pressure fluctuation on a fixed point is caused by the cavity on all of those blades, not only caused by the cavity on the blade near the point.

However, Analysis of the relations between cavitation and pressure fluctuation is still not clearly enough. There is many work need to do to study the internal mechanisms of cavitation and pressure fluctuation around the highly skewed propeller.

ACKNOWLEDGMENT

The authors are grateful to the Science and technology innovation project of Chinese Academy of Sciences through grant numbers KGFZD-125-014, national natural science foundation of china through grant numbers 11202215&11332011, and the Youth Innovation Promotion Association of CAS (2015015).

REFERENCES

[1] Watanabe T., Kawamura T., Takekoshi Y. et al., Simulation of steady and unsteady cavitation on a marine propeller using a RANS CFD code [C]. Proceedings of the Fifth International Symposium on Cavitation. Osaka, Japan. 2003.

[2] Ji B., Luo X., Peng X. et al., Numerical analysis of cavitation evolution and excited pressure fluctuation around a propeller in non-uniform wake [J]. International Journal of Multiphase Flow, 2012, 4: 13-21.

[3] Ji B., Luo X., Wang X. et al., Unsteady numerical simulation of cavitating turbulent flow around a highly skewed model marine propeller [J]. Journal of Fluids Engineering, 2011, 133(1): 011102.

[4] Hasuike N., Yamasaki S., Ando J., Numerical study on cavitation erosion risk of marine propellers operating in wake flow[C]. Proceedings of the 7th International Symposium on Cavitation. Nobuhiro Hasuike, Michigan, USA, 2009.

[5] Decaix J., and Goncalvès E., Compressible effects modeling in turbulent cavitating flows [J]. European Journal of Mechanics-B/Fluids, 2013, 39: 11-31.

[6] Goncalvès E., Numerical study of unsteady turbulent cavitating flows [J]. European Journal of Mechanics-B/Fluids, 2011. 2011, 30(1): 26-40.

[7] Wang Y. W., Liao L. Z., Du T. Z. et al., A study on the collapse of cavitation bubbles surrounding the underwater-launched projectile and its fluid–structure coupling effects[J]. Ocean Engineering, 2014, 84: 228-236.

[8] Huang B., Young Y. L., Wang G. et al., Combined experimental and computational investigation of unsteady structure of sheet/cloud cavitation [J]. Journal of fluids engineering, 2013, 135(7): 071301.

[9] Lu N. X., Svennberg U., Bark G. et al., Numerical simulations of the cavitating flow on a marine propeller [C]. Proc. 8th International Symposium on Cavitation, Claus-Dieter OHL et al., eds., Singapore, 2012, 338-343.

[10] Lu N. X., Bensow R. E., Bark G., Large Eddy Simulation for Incompressible Flows simulation of cavitation development on highly skewed propellers [J]. Journal of Marine Science and Technology, 2014, 19(2): 197-214.

[11] Bensow R. E., Bark G., Simulating cavitating flows with LES in openfoam [C]. Proc. Fifth European Conference on Computational Fluid Dynamics, J. C. F. Pereira, and A. Sequeira, eds., Lisbon, Portugal. 2010.

[12] Bensow, R. E. and Bark G., Implicit LES Predictions of the Cavitating Flow on a Propeller [J]. Journal of Fluids Engineering, 2010, 132(4): 041302.

[13] Liu D., Liu S., Wu Y. et al.,LES numerical simulation of cavitation bubble shedding on ALE 25 and ALE 15 hydrofoils [J]. Journal of Hydrodynamics, Ser. B, 2009, 21(6): 807-813.

[14] Yu X. X., Huang C. G., Du T. Z. et al., Study of characteristics of cloud cavity around axisymmetric projectile by large eddy simulation [J]. Journal of Fluids Engineering, 2014, 136(5): 051303.

[15] Huang B., Zhao Y., Wang G., Large eddy simulation of turbulent vortex-cavitation interactions in transient sheet/cloud cavitating flows [J]. Computers & Fluids, 2014, 92: 113-124.

[16] Kurobe Y., Ukon Y., Koyama K. et al., Measurement of Cavity Volume and Pressure Fluctuations on a Model of the Training Ship SEIUN-MARU With Reference to Full Scale Measurement [J]. Ship Research Institute, Technique Report No. (NAID), 1983, 110007663078.

[17] Takahashi H., Full Scale Measurements On Training Ship "SEIUN-MARU" [C]. Proc. 17th International Towing Tank Conference (ITTC 84), O. Rutgersson, eds., SSPA, Sweden, Session 1a on Full Scale Measurements, 1984, 323-334.

[18] Wu X. C., Wang Y. W., Huang C. G. et al., Effect of mesh resolution on large eddy simulation of cloud cavitating flow around a three dimensional twisted hydrofoil [J]. European Journal of Mechanics-B/Fluids, 2016, 55: 229-240.

[19] Kunz R. F., Boger D. A., Stinebring D. R. et al., A preconditioned Navier–Stokes method for two-phase flows with application to cavitation prediction [J]. Computers & Fluids, 2000, 29(8): 849-875.

[20] OpenFOAM Wep Site. http://openfoam.org/release/2-1-0/ami/. 2011.

[21]Farrell P. E., Maddison J. R., Conservative interpolation between volume meshes by local Galerkin projection[J]. Computer Methods in Applied Mechanics and Engineering, 2011, 200(1): 89-100.